Agricultural Water Management 290 (2023) 108607

Contents lists available at ScienceDirect

Agricultural Water Management

journal homepage: www.elsevier.com/locate/agwat

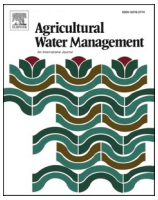

Root phenotyping and root water uptake calculation using soil water contents measured in a winter wheat field

Zhongdong Huang [a,b,*], Xiaoxian Zhang [b], Rhys W. Ashton [b], Malcom J. Hawkesford [b], W. Richard Whalley [b]

[a] Institute of Farmland Irrigation, Chinese Academy of Agricultural Sciences, Xinxiang 453002, Henan Province, PR China
[b] Rothamsted Research, Harpenden, Hertfordshire AL5 2JQ, United Kingdom

ARTICLE INFO

Handling Editor: Dr Z Xiying

Keywords:
Root water uptake
Markov Chain Monte Carlo
Bayesian inference
Root phenotyping
Winter wheat
Field experiment

ABSTRACT

Non-destructive phenotyping of roots and measurement of root water uptake from different soil layers in the field are vital for improving water management and facilitating the development of drought-resistant crop varieties, but difficult because of their opaqueness. As a result, indirect methods using easy-to-measure variables such as soil water content have been used as alternatives. However, the inherent measurement errors could undermine the robustness and reliability of these methods. This paper proposes a new method to bridge this knowledge gap by using soil water content profiles measured at two time points to calculate root uptake and root-length density. It is based on the Richards' equation by treating root uptake from different soil layers between the two time points as random unknown numbers; their distributions are calculated using the Bayesian framework, solved by the Markov Chain Monte Carlo method. We applied the method to 39 winter wheat lines grown in a silt-clay loam field. Soil water content profile measured at the first time point from each plot served as the initial condition, and water content measured at the second time point was the target to match the model for calculating average root water uptake and root-length density between the two time points. The results show that the measured soil water contents fall within the 95% confidence interval of the calculated soil water contents. The inherent soil water measurement errors lead to uncertainties in the calculated root water uptake for all lines, but such uncertainties decrease with soil depth. Although the soil types and agronomic management were the same for all 39 lines, their root water uptake from different soil layers varies considerably, with some lines more capable of using subsoil water than others. Generally, the calculated and measured root-length densities agree well, albeit the degree of the agreement varies with lines. While this paper focuses on methodology and applies the method to one growth stage spanning one month only, the consistent results for all 39 lines indicates the method is robust and can be applied to other crops cultivated in different conditions. Given the growing interest in improving root traits to enhance water use efficiency, the proposed method has important implications as phenotyping roots and understanding their water uptake from different soil layers in the field is a prerequisite to achieve this crucial target.

1. Introduction

Root water uptake is not only an important hydrological process (Beer et al., 2010; Bengough, 2012; Coenders-Gerrits et al., 2014; Jasechko et al., 2013), but also controls photosynthesis and carbon cycle in terrestrial systems. It has been used to estimate gross primary productivity of ecosystems where experimental measurements are infeasible (Beer et al., 2007; Cheng et al., 2017). While root water uptake has been studied for centuries, some issues, such as how plants adjust their water uptake from different soil layers in response to environmental change as well as the underlying mechanisms, remain elusive (Bonan et al., 2014; Chen et al., 2020; Gat, 1996; Penman and Keen, 1948; Williams et al., 2004), and processes are stilling be made (Müllers et al., 2022; Müllers et al., 2023).

Root growth and its water acquisition are jointly modulated by soil and root architecture. When the environment of root growth changes, plants adjust their root architecture and hydraulic network to facilitate water uptake to keep the water status in plant (Atkinson et al., 2020; Dunbabin et al., 2006; Zhou et al., 2020). As directly measuring roots and their water uptake is difficult in the field (Flavel et al., 2014; Rabbi

* Corresponding author at: Institute of Farmland Irrigation, Chinese Academy of Agricultural Sciences, Xinxiang 453002, Henan Province, PR China.
E-mail address: zdhuang@126.com (Z. Huang).

https://doi.org/10.1016/j.agwat.2023.108607
Received 12 July 2023; Received in revised form 16 October 2023; Accepted 22 November 2023
Available online 25 November 2023

et al., 2018; Zarebanadkouki et al., 2013), classical root phenotyping is excavation and coring-counting (Gregory et al., 1978a; Gregory et al., 1978b). To link root architecture to water uptake, various methods have been developed, among which the isotope method by simultaneously measuring stable isotopes in plant stem and along the soil profile appears to be most promising. The origin of the isotopes flowing through the stem (hence its associated water) can be tracked down to soil based on mass balance (Brooks et al., 2010; Liu et al., 2021; Ma and Song, 2016; Schwendenmann et al., 2015). While isotope method has been widely used, it neglects that the movement of isotopes from the location they are taken from soil to the location in the stem where they are sampled is not a convective process as presumed by the mass-balance method; they mixes with isotopes taken by roots from other places in the soil due to interconnectedness of the xylems and variation of water velocities in and between the xylems (Ehleringer and Dawson, 1992; Gao et al., 2020). Apart from these hydrodynamic mixings, there are other error sources that affect the isotope method (von Freyberg et al., 2020).

Spatiotemporal change in soil water content is the footprint of root water uptake and it can hence be used to interpret root traits and root water uptake (Vandoorne et al., 2012). The easiest way is soil-drying method where root water uptake from a soil layer is assumed to be the difference in soil water contents measured at two time points (Dardanelli et al., 1997; Garre et al., 2011; Müllers et al., 2023; Nelson et al., 2006). This method does not need soil parameters and works well when soil is relatively dry in that soil water change is predominantly induced by root water uptake and water redistribution induced by gravity and matric potential gradient is negligible. When vertical water flow is significant following rainfall or irrigation, however, the soil-drying method is no longer valid to estimate root water uptake (Domec et al., 2010; Zhang et al., 2021). An improvement is to include vertical water flow to inversely (or backwardly) calculate root water uptake by numerically solving the nonlinear Richards' equation with soil hydraulic properties taken as known *priori* (Angaleeswari and Ravikumar, 2019; Liao et al., 2016). Unlike forward modelling, however, inverse modelling is ill-posed in that a small measurement error could be amplified to substantial errors in the calculated root water uptake. To improve the accuracy of the inverse modelling, various methods have been developed (Guderle and Hildebrandt, 2015). All these methods calculate root water uptake by minimising the difference between measured and simulated soil water contents at some time points, and they differ only in how to achieve, iteratively, the minimisation. One simple method is to progressively update an initial water uptake estimated from the soil-drying method until a satisfactory agreement between the simulated and measured soil water contents is reached (Zuo and Zhang, 2002). Others include using modified functions to reduce the impact of measurement errors (Li and Yue, 2018). While these methods have been verified against synthesised data without errors, their application to the field is limited where soil properties and root growth are complicated, and experimental measurements are prone to errors. In fact, it has been found that the optimisation-based methods that work satisfactorily for error-free synthesised data could fail when applied to data with errors (Guderle and Hildebrandt, 2015). Instead of solving the optimization and the nonlinear Richards equation, an alternative is to directly calculate root uptake based on mass balance if soil water content can be measured accurately in high frequency such as at hourly intervals (Angaleeswari et al., 2021; Li et al., 2002). Despite the intensive research on root water uptake and the underlying mechanisms over the past decades, studies on how to deduce root-length density from root water uptake are limited.

We present a new method in this paper to calculate root water uptake and phenotype roots. Soil water movement induced by water redistribution and root uptake is modelled by the Richards' equation, and root water uptake from each soil layer is treated as an unknown random number. Its probability distribution is calculated using the Bayesian framework solved by the Markov Chain Monte Carlo (MCMC) method. Root water uptake is intricately linked to root architecture and roots in the same soil layer could compete for water with the root-length density increasing. To account for this phenomenon, root water uptake rate in each soil layer is assumed to increase asymptotically with root-length density. The method was applied to 39 winter wheat lines grown in different plots under the same management in a silt-clay loam field. For each line, we calculated its root water uptake rate and root-length density, and then compared these with ground-truth data. This allows us to gain insights into the variation among these lines in their utilization of water from different soil layers and to elucidate genetic differences between these lines in their root water uptake.

2. Materials and methods

2.1. The experiment

The field experiment was conducted from 2017 to 2018 in one of the Rothamsted long-term experiments at Woburn in the UK. It aimed to study the growth of different winter wheat lines under the same growing conditions. Soil in the experimental site is silt-clay loam, and the experiment comprised 504 separate 9 × 1.8 m plots, over which 39 winter wheat lines, each having three replicates, were sown on 10/10/2017. The field experiment was rainfed; husbandry for all lines were the same, following standard agronomic protocols for the UK with adequate fertilisation, weed, and pest and disease control. Water content profile in each plot was measured four times from 05/03/2018–11/06/2018 using the neutron probe method via an aluminium access tube installed approximately 1 m from one end of the plot.

Soil cores 100 cm long and 5 cm in diameter were taken between 4/7/18–2/8/18, when the crops were at the flowering stage, from each plot using an auger (Van Walt Ltd., Surrey, UK) at a location approximately 1 m from the aluminium tube on the side towards the plot centre. They were then stored into a black plastic bag. Root length-density was measured using core-breaking method (Hodgkinson et al., 2017), in which each core was broken at a position about 5 cm from its top surface first to reveal a fresh face; the remaining part was then broken into a number of 10 cm-long segments. The number of roots in the two end faces of each segment was counted three times, by rotating the core 120° after each counting. The number of roots in each segment was the number of roots on the two end faces; the root counts were converted into root length density assuming that the roots in each segment were parallel to the core wall (Hodgkinson et al., 2017).

Considering the sampling date of both soil water and root-length density, we used soil water measured on 15/5/2018 and 11/6/2018 in the modelling, with the former serving as the initial condition and the latter as the target to match the simulated soil water content for calculating water uptake and root-length density. Changes in daily temperature and rainfall over this period are shown in Fig. 1.

2.2. The models

The model consists of two parts. The first one is to numerically simulate soil water flow along the soil profile, with root water uptake in each soil layer taken as an unknown random number whose distribution function is solved by the Bayesian inference method. The second one is to estimate the root-length density based on the calculated root water uptake rate.

2.2.1. Water flow

Water flow and root water uptake are volumetric average over each a horizontal layer; they are described by the following Richards' equation (Richards, 1931):

$$\frac{\partial \theta}{\partial t} = \frac{\partial}{\partial z}\left[K\frac{\partial (h-z)}{\partial z}\right] - s, \tag{1}$$

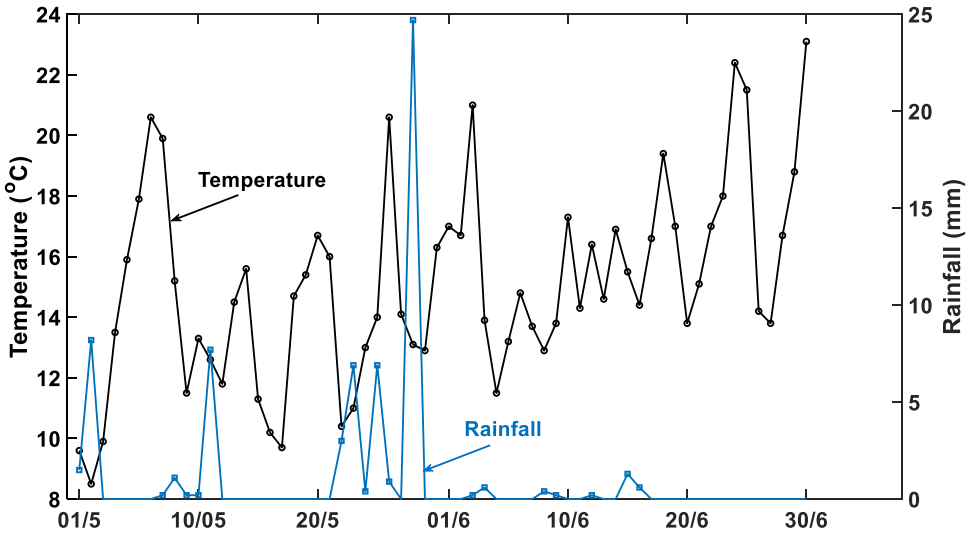

Fig. 1. Changes in daily temperature and rainfall during the studied period.

where θ is volumetric water content, t is time (day), K is hydraulic conductivity (cm/day), h is matric potential (cm), z is depth (cm), and s is root water uptake rate (1/day). Eq.(1) was solved using the method we proposed previously (Zhang et al., 2002), with the time-derivative term approximated by the method of Celia (Celia et al., 1990). Details of the numerical solution are given in the appendix. Water release curve of the soil was taken from data published previously (Gregory et al., 2010), and the hydraulic conductivity was estimated from the water release curve based on the van Genuchten formula (1980), with the saturated hydraulic conductivity estimated based on soil moisture profile measured from the experimental site.

Hydraulically, root water uptake depends on the potential difference between water in root xylems and at the root-soil interface, as well as root hydraulic conductance in both radial and longitudinal directions. In the macroscopic model, these microscopic processes were volumetrically averaged, with the root uptake rate in each horizontal layer treated as an unknown random variable.

2.2.2. Root water uptake

Soil moisture change from $t_0 = 15/5/2018$ and $t_1 = 11/6/2018$ was simulated using Eq. (1). For each soil layer we used an average to represent the root water uptake rate from t_0 to t_1. Soil moistures measured at t_0 served as the initial condition, and those measured at t_1 were the target to match the simulated moistures for calculating root water uptake. Considering the errors in the measurement and model approximation, we postulated root water uptake rate in each soil layer as a likelihood, approximating its priori distribution function by a uniform distribution and calculating its posterior distribution by the MCMC using the algorithm proposed by Lu et. al (2014). Details of the method are given in the appendix.

2.2.3. Root-length density

Experimental data measured from stable isotopes and other methods have shown that root water uptake rate increases with root-length density (Gao et al., 2022; Zhang et al., 2020), but asymptotically due to the competition of roots for water in regions where roots proliferate while bioavailable water cannot sustain root adsorption. We use the following equation to describe their asymptotic relationship:

$$s(z) = A\frac{RLD(z)}{B + RLD(z)}, \tag{2}$$

where RLD(z) is root-length density at depth z, and A and B are parameters. When roots are spatially sparse in that RLD(z)< <B, there is no competition between roots and root water uptake rate increases linearly with RLD. In contrast, in regions where roots are dense in that RLD(z)> >B, because of competition, with the increase in root-length density, the increase in root water uptake flattens. The parameter B hence represents the level of root competition.

The roots measured from the coring-counting and by others both shows that root-length density decreases with soil depth exponentially as follows (Gregory et al., 1978b; Zuo et al., 2004):

$$RLD(z) = \alpha\exp(-\beta z), \tag{3}$$

where α and β are parameters. Substituting Eq. (3) into Eq. (2) gives the relationship between root-length density and the associated water uptake:

$$s(z) = \alpha{\cdot}A\frac{\exp(-\beta z)}{B + \alpha\exp(-\beta z)}, \tag{4}$$

Fitting Eq. (4) to the root uptake rates calculated from the Bayesian framework enables us to estimate the root-length density distribution.

Soil textures in all experimental plots are approximately the same and we hence assumed that their hydraulic parameters were also the same. We acknowledge that this is an approximation, but rational as previous analysis found that root traits of all lines did not differ from each other significantly (Zhang et al., 2020). For all plots, the simulated domain extended from the soil surface to the depth of 150 cm. As leaf area index approximately peaked in June and there was no significant difference between the lines (Zhang et al., 2020), water evaporation from the soil surface was negligible compared to transpiration. The soil surface was hence treated as a zero-flux boundary for water flow. The bottom boundary was set at the depth of 150 cm where water flow was driven by gravity in that the gradient of the matric potential was zero. Since root water uptake is predominantly in the topsoil, to reduce the number of root uptake to calculate and improve reliability of the method, we used a constant to approximate the root water uptake rate in the depth from 81 to 150 cm. For each soil layer that was 10 cm thick above the depth of 80com, we used a constant to describe the average root water uptake between the two sampling time points. Overall, there were nine unknown root water uptake rates along the soil profile in each plot.

3. Results

Eq. (4) was derived based on the fact that RLD decreases with depth exponentially. To demonstrate this applies to our experiment, Fig. 2A

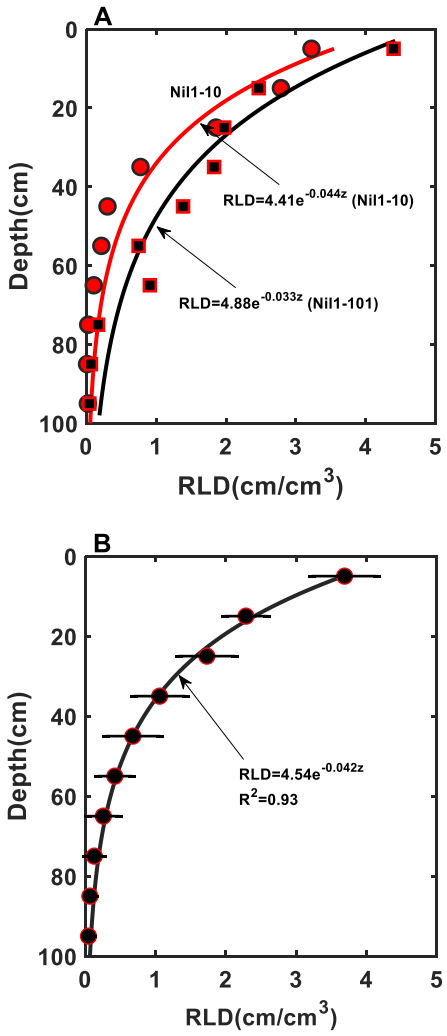

Fig. 2. The change in root-length density (RLD) with soil depth fits well to the exponential function for two randomly selected Nil1–10 and Nil1–101 (A). Fitting the average RLD of all 39 lines to an exponential function (error bars are standard errors).

shows the distribution of root-length density measured for two lines randomly selected from the 39 lines, in comparison with the fitting of the exponential function. Overall, they agree well with $R^2 = 0.95$. We also fitted the variation of the average RLD of all 39 lines with soil depth to an exponential function and show the results in Fig. 2B.

3.1. Soil water distribution

The Bayesian framework calculated by the MCM method is the posterior distribution of the root uptake rate in each soil layer, with the associated soil moisture distribution simulated by the model given in a likelihood manner bounded by a low limit and an upper limit at 95% confidence interval. The mean of the two limits can be viewed as the average soil water content. To demonstrate that the method correctly captured soil water movement, Fig. 3 compares the simulated and measured water content profiles for six plots randomly selected from the plots of the 39 lines. The results for other plots and lines are comparable to those in Fig. 3. Overall, they agree well, with most measured data falling in the envelope bounded by the low and upper limits, indicating that the method correctly reproduced root water uptake and water movement along the soil profiles.

3.2. Root water uptake distribution

The posterior distribution of root uptake rate for each layer was calculated by gradually updating a uniform prior distribution calculated based on the measured soil water content using the soil-drying method. The shape of the posterior distribution function characterises the uncertainty and mean of the water uptake rate. As an illustrative example, Fig. 4 shows the posterior distributions of the root water uptake rates at nine depths for a line randomly selected from the 39 lines after the MCMC iterations converged. To ensure that the calculated root uptake rates were physically meaningful, the low limit of the prior uniform distribution was set zero and its upper limit was 0.006 day^{-1}, a value estimated based on the maximum difference between soil water contents measured from the two time points in all plots. In general, the narrower the posterior distribution is, the less uncertain the calculated root water uptake is. Fig. 4 thus indicates that the uncertainty of the calculated root water uptake varies with soil depth; it is higher in the topsoil than in the subsoil.

Fig. 5 shows the mean root water uptake rates at different depths for the six lines in Fig. 3. Generally, the water uptake rate decreases with soil depth, consistent with the RLD distribution shown in Fig. 2. However, there are intriguing differences between the lines. For example, the lines in Fig. 5B and E took more water from the subsoil than others to sustain their transpiration.

3.3. Root-length density

RLD distribution in all plots were estimated by fitting Eq. (4) to the calculated root water uptake at different depths. As an illustrative example, Fig. 6 compares the fitting for the six lines in Fig. 5. The values of the parameters giving the best fitting in Fig. 6 are summarised in Table 1. They agree well on average, albeit the values of the parameters, especially α/B that controls the nonlinearity of the relationship between RLD and the associated root water uptake, vary between the lines.

4. Discussion

One challenge facing root water uptake measurement and root phenotyping in the field is the inherent errors associated with measurements and mathematical models (Vrugt et al., 2003). Such errors could be amplified in inverse modelling, making models that work well for error-free synthesised data fail to calculate root water uptake in the field (Guderle and Hildebrandt, 2015). The Bayesian framework treats root uptake rate from each layer as an unknown random number and calculates its distribution by the MCMC; it hence naturally captures such errors. We combined it with numerical solutions of the Richards' equation to calculate root water uptake and deduce root-length density based on soil moisture profiles measured at two time points. Application to 39 winter wheat lines cultivated in a silt-clay loam field reveals that it reproduces the root-length density reasonably well, and that the calculated root water uptake shows a subtle difference between the lines. It needs to point out that, unlike well-controlled column experiments or synthesised data used by others (Li and Yue, 2018; Zuo and Zhang, 2002), data measured from the field are prone to errors. The consistency in results for all 39 lines thus indicates that the proposed model is robust and reliable.

4.1. Root water uptake

Macroscopic models for simulating water flow treat root water uptake from each soil layer as a sink term determined by RLD and matric potential (Feddes et al., 1976; Jarvis, 1989; Molz, 1981). Some also consider compensative water uptake by roots in moist and dry regions (Thomas et al., 2020; Vandoorne et al., 2012). Unlike these models, the proposed method is to calculate root water uptake rather than simulating it. Each soil profile was divided into nine layers. This is not only to

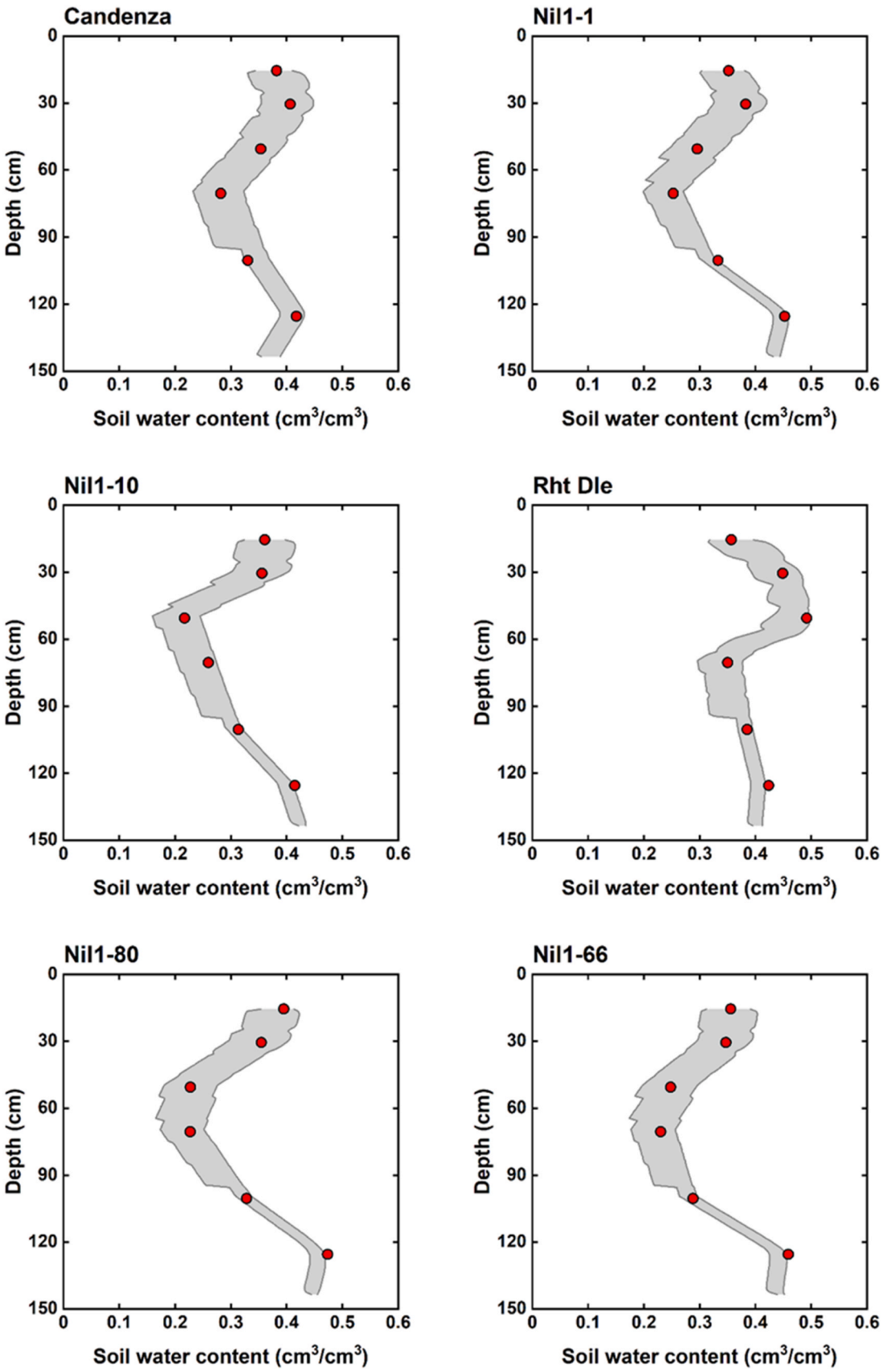

Fig. 3. Comparison between the measured soil water content (symbols) and the areas bounded by the 95% confidence interval of the soil water content simulated using the Bayesian framework for six lines randomly selected from the 39 lines.

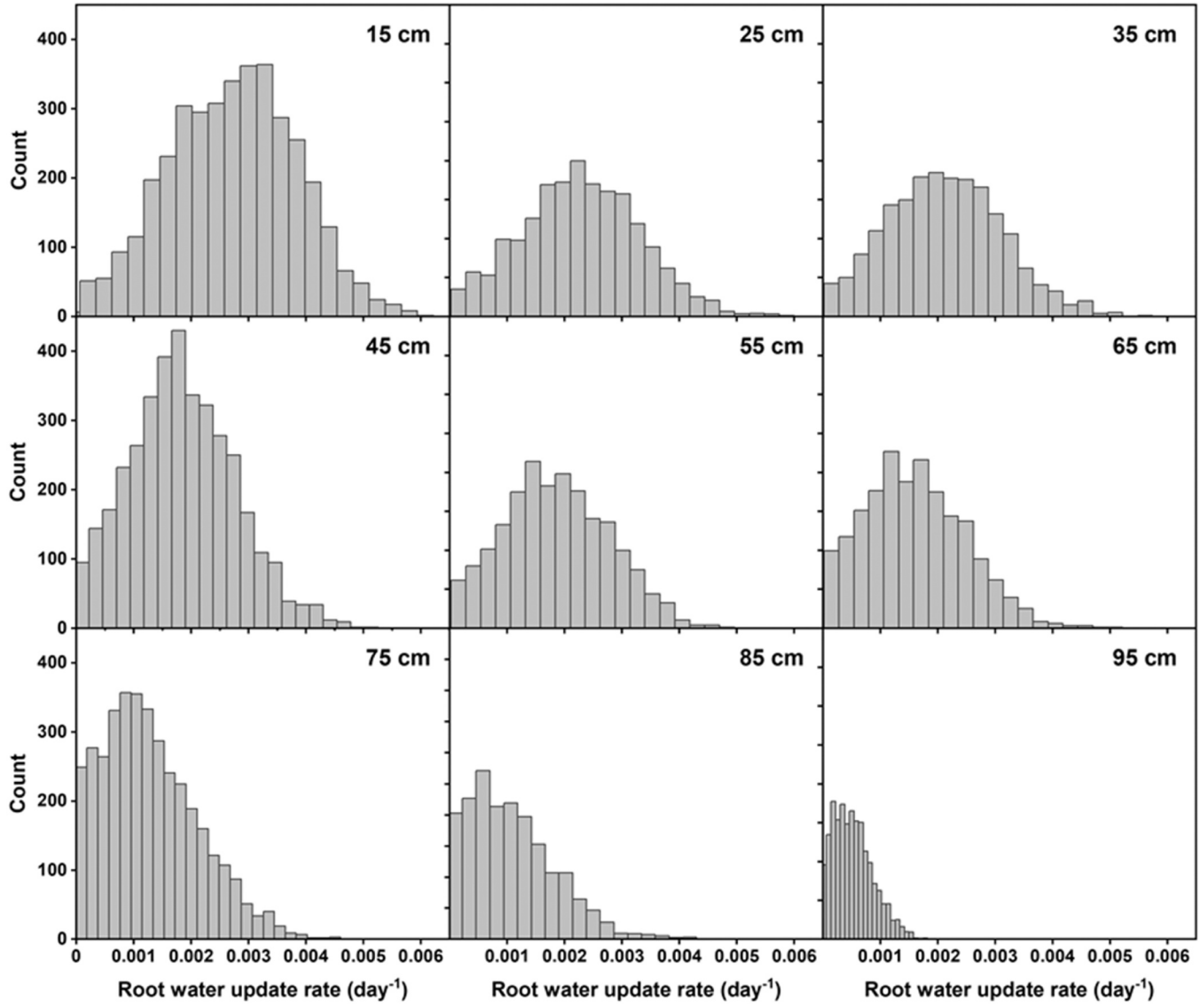

Fig. 4. Illustrative examples showing the posterior distributions of root water uptake in the nine soil layers calculated from the MCMC model for one plot grown with Candenza line. Results (not presented) for other plots and lines are similar.

reduce the number of root water uptake rates to calculate, but also due to physical consideration that soil water content measured by the neutron probe is not a point-value but an average around the location where the neutron probe is located in making the measurement.

Previous studies have shown that the location of maximum root uptake rate shifted in soil profile as soil water content in the profile changed (Li et al., 2002), while our results indicate that the average root uptake of all lines peaked in the topsoil (Fig. 5). Hydraulically, root water uptake is controlled by water potential difference between root xylems and the root-water interface, but how much water the roots can take up depends on the bioavailable water in each soil layer. Coarse-textured soils such as the sand used in the experiment of Li et al. (2002) normally are associated with low porosity (0.378) and high hydraulic conductivity, in which root uptake and gravity-driven flow can quickly dry the topsoil, making shallow roots under water stress. As a result, roots increase their water uptake from the subsoil to sustain transpiration. In contrast, fine-textured soils like that in our experiment are characterised by high porosity (0.56) and low hydraulic conductivity, where water in the topsoil could be sufficient for roots to adsorb even when the topsoil is relatively dry (Gregory et al., 2010), as manifested in the soil moisture distribution measured in the field (Fig. 3).

Previous analysis did not show significant differences in root-length density and leaf index between the lines (Zhang et al., 2020), but this does not transfer to root water uptake. For example, root water uptake of the lines in Figs. 5B and 4E differ considerably from other lines, indicating that apart from root traits, other factors also play an important role in water uptake, albeit we cannot identify what these factors are. One possible mechanism is soil structure and mucilage exudated by roots into the rhizosphere which modulate root water uptake but differ between the lines (Schwartz et al., 2016; Zhang et al., 2020). Another one is the variation in radial root hydraulic conductance between different lines in their response to environmental change. In fact, a recent study found significant genetic variations in radial hydraulic conductivity of 224 maize inbred lines (Rishmawi et al., 2023). The importance of root traits in water uptake has been intensively studied over the past decades (Javaux et al., 2013; Lynch, 2013; Lynch, 2019; Postma et al., 2014), but Fig. 5 shows that other factors are equally important in mediating root water uptake and should be considered in screening drought-tolerant varieties (Gao et al., 2020; Sun et al., 2021; Wang et al., 2020).

One advantage of the Bayesian framework method is that it considers measurement errors and their consequence for root water uptake

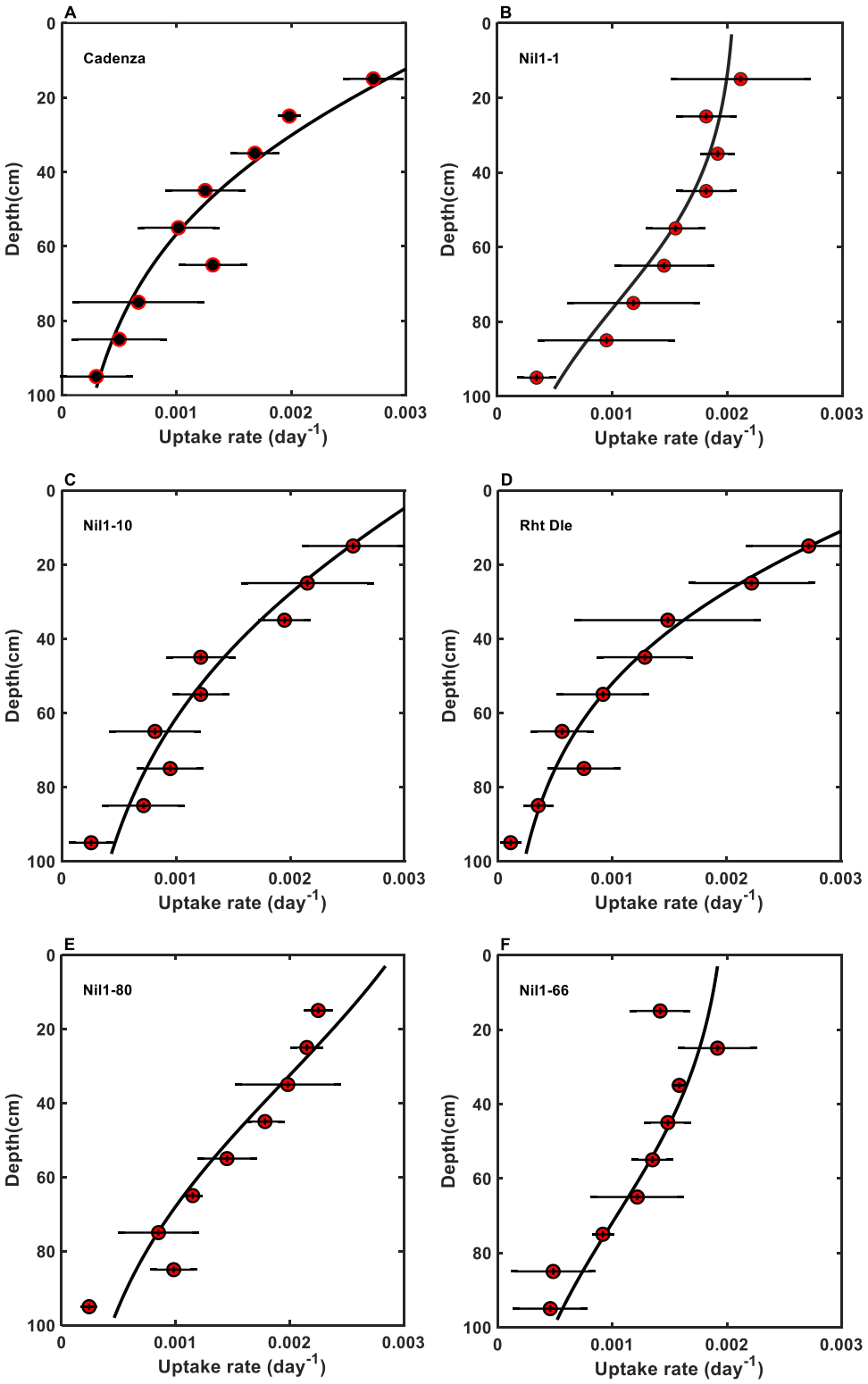

Fig. 5. Comparison between root water uptake calculated from the MCMC method (symbols) with the best fitting (solid lines) of Eq. (4) using the parameters in Table 1 for the six lines shown in Fig. 3. The error bars represent the average of the replicas for each line.

calculated for each soil layer (Fig. 4). The distributions of root water uptake rates calculated for all lines are bell-shaped, and its shape changes gradually from approximately normal distributions for the topsoil to skewed distributions for the subsoil. Their associated uncertainties decrease with soil depth because water content measured from the topsoil was more erroneous than that from the subsoil (Fig. 5).

4.2. *Root-length density*

Apart from soil water content, root water uptake is also regulated by root architecture and their radial and axial hydraulic conductance (Javaux et al., 2013). For subsoil where roots are sparse and soil is moist, roots do not compete for water and the total root water uptake from the

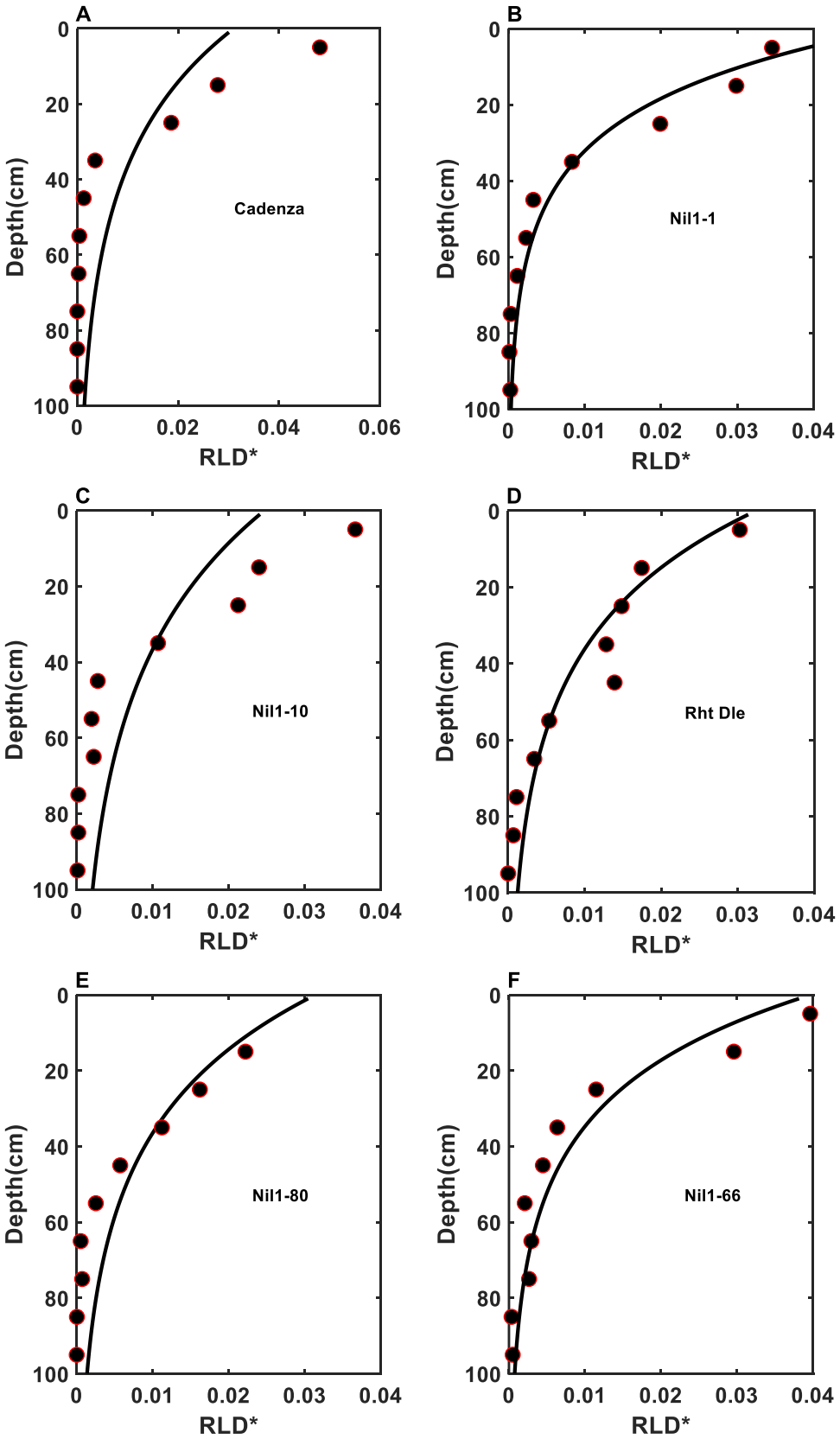

Fig. 6. Comparison between the measured root-length density (symbols) and estimated from Eq. (4) based on the average root uptake rates calculated (solid lines) for the six lines shown in Fig. 5.

Table 1
The best-fitting parameters of Eq. (4) for matching root water uptake rates of the six lines shown in Fig. 5.

	Cadenza	Nil1-1	Nil1-10	Rht Dle	Nil1-80	Nil1-66
A (day^{-1})	0.0092	0.0021	0.0085	0.0107	0.0039	0.0021
β (cm^{-1})	0.031	0.051	0.025	0.032	0.031	0.040
α/B	0.71	42.99	0.61	0.55	2.89	16.51

subsoil layers hence increases linearly with root length (Ma and Song, 2016; Xu et al., 2021). In the topsoil, roots are densely distributed and compete for water. The depletion of water by each root creates a local matric potential gradient which expands radially from the root as time elapses. If the depleted water cannot be replenished by irrigation or rainfall timely, the depletion zones created by adjacent roots overlap, leading to root competition for water. Therefore, root water uptake from the topsoil tends to flatten as the root-length density increases. Water potential difference between the topsoil and subsoil can drive subsoil water moving upwards, especially in evening when root uptake ceases, to partly replenish the lost water in the topsoil to avoid severe water stress (Zuo et al., 2006). The close relationship (R^2 >0.9) between the measured and calculated root-length density for all lines as illustrated in Fig. 6 indicates that Eq. (4) is rational and consistent with above analysis and other studies (Corneo et al., 2018; Lv et al., 2010).

Process-based models such as HUDURUS and SWAP simulate the reduced root water uptake due to root competition by a compensatory function (Hartmann et al., 2018; Li et al., 2001; Simunek and Hopmans, 2009). This paper is not to simulate soil water flow; rather it is to calculate root water uptake and deduce root traits using soil water profiles measured at two time points, as change in soil water content between the two time points is the footprint of root water uptake. The reduced root water uptake due to root competition is described by the pre-defined Michaelis-Menten type function (Eq. 4). Fig. 5 indicates that it captures the change in root water uptake with soil depth reasonably well. Root uptake in Fig. 5 is averages over the two sampling points rather than values at any specific time. While water uptake by roots in different soil layers is dynamic and varies instantly following a change in environment (Maurel et al., 2010; Rishmawi et al., 2023), for phenotyping roots and identifying the difference in root water uptake between different varieties in the field, the proposed method for calculating average root water uptake over two sampling time points is sufficient.

Eq. (4) has four parameters but α and B can be combined. Therefore, there are only three independent parameters, including the root-length distribution parameter β. To validate Eq. (4), we normalise the root-length density measured at each depth by the total root length measured across the soil profile, that is, $RLD*(z) = RLD(z)/\int_0^\infty RLD(z)dz$, to compare the root length density estimated from the root water uptake via Eq. (4) with that directly measured from 4/7/18–2/8/18. The agreement varies with lines and as an illustration, Fig. 6 compares six lines randomly selected from the 39 lines; the results for other lines are comparable to those in Fig. 6. The values of the parameters in Eq. (4) are summarised in Table 1.

There are discrepancies between the measured and calculated root-length density. Apart from the inherent errors induced by Eq. (4), there are other error sources. One is the coring-counting method itself, which could have missed some fine roots not exposed to the end faces of the segments. The measured root-length density is comparable to those obtained using the similar method by others (Gregory et al., 1978b; Lv et al., 2010), but is less than that measured using soil-washing, suggesting that root-counting misses roots. The second is that root distribution in the field is spatially heterogeneous, and roots in a 10 cm x 5 cm core might not be representative of the roots in soil where the aluminium access tube was installed, especially in the deep soil where the roots were sparse. There is a systemic difference between the calculated and measured root-length densities, with the former underestimating the roots in the topsoil while overestimating the roots in the subsoil (Fig. 6). While this could be due to measurement and model errors, another reason is that the roots estimated by the model are roots that actively take up water. Such roots could penetrate as deep as 2 m (Thorup-Kristensen et al., 2009), which were likely to have been missed in the coring-counting but captured in the model. Also, root water uptake varies with root age (van Dusschoten et al., 2020), and roots in the topsoil are relatively aged and some, identified in the core counting, might not be very active in absorbing water.

4.3. Difference between lines in their water uptake

The penetration depth and the variation of root density with depth is collectively represented by the parameter β in Eq. (4). The competition of roots in the same soil layer is represented by α/B. These parameters can be used as proxies to distinguish the genetic difference between the lines in their efficacy to take up water. For doing so, we use the function $\tau = \exp(-\beta z)$ as a proxy for root length at the depth of z, which varies with lines (Table 1). The change in root water uptake with the proxy root length can thus be written as $S = M{\cdot}\tau/[1+\alpha/B{\cdot}\tau]$ where M=A·α/B. When α/B = 0, S is proportional to τ, meaning that roots do not compete for water. Physically, the derivative of S to τ (i.e., $F' = \partial S/\partial\tau$) represents the increasing rate in root water uptake with the increase in root length. In simpler terms, it represents how effectively a crop can enhance its water uptake by growing more roots. Because of the difference in parameters M and τ between the lines (Table 1), there is a salient difference between the lines in their efficiency of taking up water. As a demonstrating example, we take three lines from Fig. 5 and compare the increase of their F' with τ in Fig. 7. The rapid increase in F' with τ for the Candenza line indicates that a slight increase in its root length leads to a greater increase in its water uptake than a similar increase in root length of the Nil-66 line, whose F' increases more slowly with τ. In other words, the roots of the Candenza line are more effective than the roots of Nil-66 line in taking up water, consistent with previous studies that lines with statistically similar root morphology could have very different root water uptake capacity (Zhang et al., 2020). The underlying mechanisms could be physiological, biophysical, or their combination. Physiologically, it could be due to genetic difference in root hydraulic conductivity of different lines (Rishmawi et al., 2023), which control water flow from root-soil surface to the xylem vessels and its subsequent ascent. Biophysically, different lines might have different rhizosphere which mediates the ability of the rhizosphere to hold water and water movement from distant soil into the rhizosphere (Helliwell et al., 2019; Rabbi et al., 2018; Zhang et al., 2020). This work cannot untangle these mechanisms, but reveals that relying on root morphology alone is inadequate to assess root uptake, and biophysical and root hydraulic traits also play a significant role and should be included in breeding and screening drought-tolerance varieties (Hallett et al., 2022; Rishmawi et al., 2023).

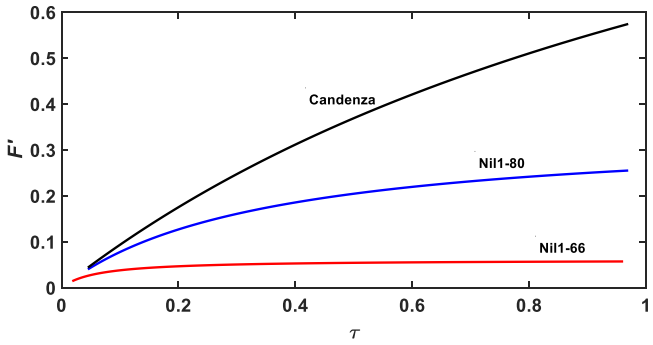

Fig. 7. Illustrative examples showing the difference between lines in the efficiency of their roots in taking up water. Higher F' corresponds to faster increase in root water take as root length increases, meaning greater efficiency of roots in taking up water.

5. Conclusions

Measuring root water uptake and phenotyping roots in the field are challenging. The existing indirect methods using easy-to-measure soil moisture to estimate root uptake take could fail due to the inherent measurement errors. We combine the Richards' equation and the Bayesian inference to quantify these uncertainties by treating root water uptake from each soil layer as an unknown random number. Its distribution is solved by the Markov Chain Monte Carlo method, from which we deduce the root length density. Application of the method to 39 winter wheat lines grown in a field indicates that the root-length density calculated for all lines agree reasonably well with ground-truth data, albeit the degree of the agreement varies with lines. We found that there are significant differences between these lines in their ability and efficiency to take up water from different soil layers, with some lines more effective in using subsoil water while some lines more efficient in taking up soil water. This suggests that root-length density alone is insufficient to assess root water uptake and other biophysical and physiological traits also play an important role and should be considered in screening drought-tolerant varieties. Although we only calculated one growing stage, the consistent results for all 39 lines indicate that the method is robust and reliable. It can also be applied to other crops cultivated in different conditions.

Declaration of Competing Interest

We declare that we have no financial and personal relationships with other people or organizations that can inappropriately influence our work, there is no professional or other personal interest of any nature or kind in any product, service and/or company that could be construed as influencing the position presented in, or the review of, the manuscript entitled.

Data Availability

No data was used for the research described in the article.

Acknowledgments

Rothamsted Research receives funding from the Biotechnology and Biological Sciences Research Council (BBSRC), including the Delivering Sustainable Wheat (BB/X011003/1, BB/P016855/1) Institute Strategic Programme. ZDH is funded by the National Key Research and Development Program of China (No. 2022YFF0711804) and the Central Public-interest Scientific Institution Basal Research Fund (No. Y2021YJ26). The computer codes are available from the corresponding authors on request.

Appendix

A1. Numerical solutions

We solve Eq. (1) numerically based on the method we proposed previously (Zhang et al., 2002) with the time derivative solved by the method of Celia et al. (1990).

$$\frac{(z_{i+1}-z_{i-1})}{2}\frac{\theta_i^{t+\delta t}-\theta_i^t}{\delta t}=K_{i+1/2}^{t+\delta t}\frac{h_{i+1}^{t+\delta t}-h_i^{t+\delta t}}{z_{i+1}-z_i}+K_{i-1/2}^{t+\delta t}\frac{h_{i-1}^{t+\delta t}-h_i^{t+\delta t}}{z_i-z_{i-1}}+K_{i-1/2}^{t}-K_{i+1/2}^{t}-s_i^{t+\delta t/2}, \tag{A1}$$

where z_{i-1}, z_i and z_{i+1} are the coordinates of numerical nodes, δt is a time step, the superscripts t and $t+\delta t$ represent the value at the two time points respectively, and subscripts i-1, i and i + 1 represent the values at location z_{i-1}, z_i and z_{i+1} respectively. The above nonlinear equation was solved using following iterative methods:

$$\begin{aligned}
&\frac{\Theta_i}{\delta t}h_i^{t+\delta t,m+1}+A_i\left(h_i^{t+\delta t,m+1}-h_{i+1}^{t+\delta t,m+1}\right)-B_i\left(h_i^{t+\delta t,m+1}-h_{i-1}^{t+\delta t,m+1}\right)+C_i\left(h_{i+1}^{t+\delta t,m+1}-K_{i-1}^{t+\delta t,m+1}\right)=\frac{\theta_i^{t+\delta t,m}-\theta_i^t}{\delta t}-s_i^{t+\delta t/2},\\
&\Theta_i=\left.\frac{\partial\theta}{\partial h}\right|_{h=h_i^{t+\delta t,m}}\\
&A_i=\frac{2K_{i+1/2}^{t+\delta t,m}}{(z_{i+1}-z_{i-1})(z_{i+1}-z_i)},\\
&A_i=\frac{2K_{i+1/2}^{t+\delta t,m}}{(z_{i+1}-z_{i-1})(z_i-z_{i-1})},\\
&C_i=2\frac{K_{i-1/2}^{t+\delta t,m}-K_{i+1/2}^{t+\delta t,m}}{h_{i-1}^{t+\delta t,m}-h_{i+1}^{t+\delta t,m}}.
\end{aligned} \tag{A2}$$

A2. Markov Chain Monte Carlo Bayesian inference method

We calculated the root water uptake from each soil layer using the Bayesian inference method to obtain the most likelihood water uptake rate rather than the exact water uptake rate due to the errors and uncertainties induced by field measurements and model approximation. Given a set of measured soil water contents $\boldsymbol{Y}$, the Bayesian formalism for estimating the root uptake rate in all layers $\boldsymbol{f}$ is postulated as follows:

$$p(\mathrm{f}|\mathrm{Y})=\frac{p(\mathrm{f})p(\mathrm{Y}|\mathrm{f})}{p(\mathrm{Y})}\propto p(\mathrm{f})L(\mathrm{f}|\mathrm{Y}), \tag{A3}$$

where$p(\mathrm{f}|\mathrm{Y})$and$p(\mathrm{f})$represent the posterior and prior distributions of $\boldsymbol{f}$,$p(\mathrm{Y}|\mathrm{f})$and$p(Y)$are the posterior and priori distribution of the measured soil water contents, and$L(\mathrm{f}|\mathrm{Y})$ is the likelihood function which can be estimated using the measured data as follows assuming that the measured soil water contents were normally distributed

$$L(\mathrm{f}|\mathrm{Y}) = \prod_{t=1}^{N} \frac{1}{\sqrt{2\pi\sigma_t^2}} \exp\left[\frac{1}{2\sigma_t^2}\left(\frac{y_t - y_t(\mathrm{f})}{\sigma_t}\right)^2\right], \tag{A4}$$

where y_t and $y_t(\mathrm{f})$ are the measured and simulated soil water content respectively, and σ_t^2 is the variance. The posterior distribution of the root water uptake in all layers as defined in Eq. (A3) was calculated numerically using the Monte Carlo Markov method. For MCMC sampling, we used the code of Lu et al. (2014), which was developed based on the differential evolution adaptive Metropolis (DREAM) algorithm. It was coupled with the code for numerical solution of the Richards' equation to generate the posterior distribution for each root water uptake. For each plot, five parallel chains were used to search the parameter space to approximate the posterior distribution. Convergence of the MCMC was the Gelman-Rubin (GR) criterion, deemed to have reached once GR was below 1.2. After convergence, we continue to obtain a further 7500 samples for each chain which were used to calculate the posterior distribution.

References

Angaleeswari, M., Ravikumar, V., 2019. Estimating evapotranspiration parameters by inverse modelling and non-linear optimization. Agric. Water Manag. 223, 20. https://doi.org/10.1016/j.agwat.2019.06.016.

Angaleeswari, M., Ravikumar, V., Kannan, S.V., 2021. Evapotranspiration estimation by inverse soil water flow modelling. Irrig. Sci. 39 (5), 633–649. https://doi.org/10.1007/s00271-021-00734-2.

Atkinson, J.A., Hawkesford, M.J., Whalley, W.R., Zhou, H., Mooney, S.J., 2020. Soil strength influences wheat root interactions with soil macropores. Plant Cell Environ. 43 (1), 235–245. https://doi.org/10.1111/pce.13659.

Beer, C., et al., 2010. Terrestrial gross carbon dioxide uptake: global distribution and covariation with climate. Science 329 (5993), 834–838. https://doi.org/10.1126/science.1184984.

Beer, C., Reichstein, M., Ciais, P., Farquhar, G.D., Papale, D., 2007. Mean annual GPP of Europe derived from its water balance. Geophys. Res. Lett. 34 (5) https://doi.org/10.1029/2006gl029006.

Bengough, A.G., 2012. Water dynamics of the root zone: rhizosphere biophysics and its control on soil hydrology. Vadose Zone J. 11 (2), 6. https://doi.org/10.2136/vzj2011.0111.

Bonan, G.B., Williams, M., Fisher, R.A., Oleson, K.W., 2014. Modeling stomatal conductance in the earth system: linking leaf water-use efficiency and water transport along the soil-plant-atmosphere continuum. Geosci. Model Dev. 7 (5), 2193–2222. https://doi.org/10.5194/gmd-7-2193-2014.

Brooks, J.R., Barnard, H.R., Coulombe, R., McDonnell, J.J., 2010. Ecohydrologic separation of water between trees and streams in a Mediterranean climate. Nat. Geosci. 3 (2), 100. https://doi.org/10.1038/ngeo722.

Celia, M.A., Bouloutas, E.T., Zarba, R.L., 1990. A general mass-conservative numerical solution for the unsaturated flow equation. Water Resour. Res. 26 (7), 1483–1496. https://doi.org/10.1029/WR026i007p01483.

Chen, H., Huang, J.J., McBean, E., 2020. Partitioning of daily evapotranspiration using a modified shuttleworth-wallace model, random Forest and support vector regression, for a cabbage farmland. Agric. Water Manag. 228, 12. https://doi.org/10.1016/j.agwat.2019.105923.

Cheng, L., et al., 2017. Recent increases in terrestrial carbon uptake at little cost to the water cycle. Nat. Commun. 8, 10. https://doi.org/10.1038/s41467-017-00114-5.

Coenders-Gerrits, A.M.J., et al., 2014. Uncertainties in transpiration estimates. Nature 506 (7487), E1–E2. https://doi.org/10.1038/nature12925.

Corneo, P.E., et al., 2018. Studying root water uptake of wheat genotypes in different soils using water delta O-18 stable isotopes. Agric. Ecosyst. Environ. 264, 119–129. https://doi.org/10.1016/j.agee.2018.05.007.

Dardanelli, J.L., Bachmeier, O.A., Sereno, R., Gil, R., 1997. Rooting depth and soil water extraction patterns of different crops in a silty loam Haplustoll. Field Crop. Res. 54 (1), 29–38. https://doi.org/10.1016/s0378-4290(97)00017-8.

Domec, J.C., et al., 2010. Hydraulic redistribution of soil water by roots affects whole-stand evapotranspiration and net ecosystem carbon exchange. N. Phytol. 187 (1), 171–183. https://doi.org/10.1111/j.1469-8137.2010.03245.x.

Dunbabin, V.M., McDermott, S., Bengough, A.G., 2006. Upscaling from rhizosphere to whole root system: modelling the effects of phospholipid surfactants on water and nutrient uptake. Plant Soil 283 (1–2), 57–72. https://doi.org/10.1007/s11104-005-0866-y.

Ehleringer, J.R., Dawson, T.E., 1992. Water uptake by plants: perspectives from stable isotope composition. Plant Cell Environ. 15 (9), 1073–1082. https://doi.org/10.1111/j.1365-3040.1992.tb01657.x.

Feddes, R.A., Kowalik, P., Kolinskamalinka, K., Zaradny, H., 1976. Simulation of field water uptake by plants using a soil-water dependent root extraction function. J. Hydrol. 31 (1–2), 13–26. https://doi.org/10.1016/0022-1694(76)90017-2.

Flavel, R.J., Guppy, C.N., Tighe, M.K., Watt, M., Young, I.M., 2014. Quantifying the response of wheat (Triticum aestivum L) root system architecture to phosphorus in an Oxisol. Plant Soil 385 (1–2), 303–310. https://doi.org/10.1007/s11104-014-2191-9.

von Freyberg, J., Allen, S.T., Grossiord, C., Dawson, T.E., 2020. Plant and root-zone water isotopes are difficult to measure, explain, and predict: some practical recommendations for determining plant water sources. Methods Ecol. Evol. 11 (11), 1352–1367. https://doi.org/10.1111/2041-210x.13461.

Gao, Y., et al., 2022. Different responses in root water uptake of summer maize to planting density and nitrogen fertilization. Front. Plant Sci. 13, 918043 https://doi.org/10.3389/fpls.2022.918043.

Gao, Y., Yang, Z.J., Wang, G.S., Sun, J.S., Zhang, X.X., 2020. Discerning the difference between lumens and scalariform perforation plates in impeding water flow in single xylem vessels and vessel networks in cotton. Front. Plant Sci. 11 https://doi.org/10.3389/fpls.2020.00246.

Garre, S., Javaux, M., Vanderborght, J., Pages, L., Vereecken, H., 2011. Three-dimensional electrical resistivity tomography to monitor root zone water dynamics. Vadose Zone J. 10 (1), 412–424. https://doi.org/10.2136/vzj2010.0079.

Gat, J.R., 1996. Oxygen and hydrogen isotopes in the hydrologic cycle. Annu. Rev. Earth Planet. Sci. 24, 225–262. https://doi.org/10.1146/annurev.earth.24.1.225.

Gregory, A.S., Bird, N.R.A., Whalley, W.R., Matthews, G.P., Young, I.M., 2010. Deformation and shrinkage effects on the soil water release characteristic (DOI:). Soil Sci. Soc. Am. J. 74 (4), 1104–1112. https://doi.org/10.2136/sssaj2009.0278.

Gregory, P.J., McGowan, M., Biscoe, P.V., 1978a. Water relations of winter wheat. 2. Soil-water relations. J. Agric. Sci. 91 (AUG), 103–116. https://doi.org/10.1017/s0021859600056665.

Gregory, P.J., McGowan, M., Biscoe, P.V., Hunter, B., 1978b. Water relations of winter wheat.1. Growth of root system. & J. Agric. Sci. 91 (AUG), 91. https://doi.org/10.1017/s0021859600056653.

Guderle, M., Hildebrandt, A., 2015. Using measured soil water contents to estimate evapotranspiration and root water uptake profiles - a comparative study. Hydrol. Earth Syst. Sci. 19 (1), 409–425. https://doi.org/10.5194/hess-19-409-2015.

Hallett, P.D., et al., 2022. Building soil sustainability from root-soil interface traits. Trends Plant Sci. 27 (7), 688–698. https://doi.org/10.1016/j.tplants.2022.01.010.

Hartmann, A., Simunek, J., Aidoo, M.K., Seidel, S.J., Lazarovitch, N., 2018. Implementation and application of a root growth module in HYDRUS. Vadose Zone J. 17 (1), 16. https://doi.org/10.2136/vzj2017.02.0040.

Helliwell, J.R., Sturrock, C.J., Miller, A.J., Whalley, W.R., Mooney, S.J., 2019. The role of plant species and soil condition in the structural development of the rhizosphere. Plant Cell Environ. 42 (6), 1974–1986. https://doi.org/10.1111/pce.13529.

Hodgkinson, L., et al., 2017. Root growth in field-grown winter wheat: Some effects of soil conditions, season and genotype. Eur. J. Agron. 91, 74–83. https://doi.org/10.1016/j.eja.2017.09.014.

Jarvis, N.J., 1989. A simple emperical model of root water uptake. J. Hydrol. 107 (1–4), 57–72. https://doi.org/10.1016/0022-1694(89)90050-4.

Jasechko, S., et al., 2013. Terrestrial water fluxes dominated by transpiration (+. DOI:). Nature 496 (7445), 347. https://doi.org/10.1038/nature11983.

Javaux, M., Couvreur, V., Vanderborght, J., Vereecken, H., 2013. Root water uptake: from three-dimensional biophysical processes to macroscopic modeling approaches. Vadose Zone J. 12 (4), 16. https://doi.org/10.2136/vzj2013.02.0042.

Li, K.Y., De Jong, R., Boisvert, J.B., 2001. An exponential root-water-uptake model with water stress compensation. J. Hydrol. 252 (1–4), 189–204. https://doi.org/10.1016/s0022-1694(01)00456-5.

Li, N., Yue, X.Y., 2018. Calibrating the spatiotemporal root density distribution for macroscopic water uptake models using tikhonov regularization. Water Resour. Res. 54 (3), 1781–1795. https://doi.org/10.1002/2017wr020452.

Li, Y., Fuchs, M., Cohen, S., Cohen, Y., Wallach, R., 2002. Water uptake profile response of corn to soil moisture depletion. Plant Cell Environ. 25 (4), 491–500. https://doi.org/10.1046/j.1365-3040.2002.00825.x.

Liao, R.K., Yang, P.L., Wu, W.Y., Ren, S.M., 2016. An inverse method to estimate the root water uptake source-sink term in soil water transport equation under the effect of superabsorbent polymer. PLoS One 11 (8), 17. https://doi.org/10.1371/journal.pone.0159936.

Liu, J.M., et al., 2021. Using stable isotopes to quantify root water uptake under a new planting pattern of high-low seed beds cultivation in winter wheat. Soil Tillage Res 205. https://doi.org/10.1016/j.still.2020.104816.

Lu, D., Ye, M., Hill, M.C., Poeter, E.P., Curtis, G.P., 2014. A computer program for uncertainty analysis integrating regression and Bayesian methods. Environ. Modell. Softw. 60, 45–56. https://doi.org/10.1016/j.envsoft.2014.06.002.

Lv, G.H., Kang, Y.H., Li, L., Wan, S.Q., 2010. Effect of irrigation methods on root development and profile soil water uptake in winter wheat. Irrig. Sci. 28 (5), 387–398. https://doi.org/10.1007/s00271-009-0200-1.

Lynch, J.P., 2013. Steep, cheap and deep: an ideotype to optimize water and N acquisition by maize root systems. Ann. Bot. 112 (2), 347–357. https://doi.org/10.1093/aob/mcs293.

Lynch, J.P., 2019. Root phenotypes for improved nutrient capture: an underexploited opportunity for global agriculture. N. Phytol. 223 (2), 548–564. https://doi.org/10.1111/nph.15738.

Ma, Y., Song, X., 2016. Using stable isotopes to determine seasonal variations in water uptake of summer maize under different fertilization treatments. Sci. Total Environ. 550, 471–483. https://doi.org/10.1016/j.scitotenv.2016.01.148.

Maurel, C., Simonneau, T., Sutka, M., 2010. The significance of roots as hydraulic rheostats. J. Exp. Bot. 61 (12), 3191–3198. https://doi.org/10.1093/jxb/erq150.
Molz, F.J., 1981. Models of water transport in the soil-plant system- a review. Water Resour. Res. 17 (5), 1245–1260. https://doi.org/10.1029/WR017i005p01245.
Müllers, Y., et al., 2022. Shallow roots of different crops have greater water uptake rates per unit length than deep roots in well-watered soil. Plant Soil 481 (1), 475–493. https://doi.org/10.1007/s11104-022-05650-8.
Müllers, Y., Postma, J.A., Poorter, H., van Dusschoten, D., 2023. Deep-water uptake under drought improved due to locally increased root conductivity in maize, but not in faba bean. Plant, Cell Environ. 46 (7), 2046–2060. https://doi.org/10.1111/pce.14587.
Nelson, P.N., Banabas, M., Scotter, D.R., Webb, M.J., 2006. Using soil water depletion to measure spatial distribution of root activity in oil palm (Elaeis guineensis Jacq.) plantations. Plant Soil 286 (1–2), 109–121. https://doi.org/10.1007/s11104-006-9030-6.
Penman, H.L., Keen, B.A., 1948. Natural evaporation from open water, bare soil and grass (DOI:doi). Proc. R. Soc. Lond. Ser. A. Math. Phys. Sci. 193 (1032), 120–145. https://doi.org/10.1098/rspa.1948.0037.
Postma, J.A., Schurr, U., Fiorani, F., 2014. Dynamic root growth and architecture responses to limiting nutrient availability: linking physiological models and experimentation. Biotechnol. Adv. 32 (1), 53–65. https://doi.org/10.1016/j.biotechadv.2013.08.019.
Rabbi, S.M.F., et al., 2018. Plant roots redesign the rhizosphere to alter the three-dimensional physical architecture and water dynamics. N. Phytol. 219 (2), 542–550. https://doi.org/10.1111/nph.15213.
Richards, L.A., 1931. Capillary conduction of liquids through porous mediums. Phys. -J. Gen. Appl. Phys. 1 (1), 318–333. https://doi.org/10.1063/1.1745010.
Rishmawi, L., et al., 2023. Natural variation of maize root hydraulic architecture underlies highly diverse water uptake capacities. Plant Physiol. 15 https://doi.org/10.1093/plphys/kiad213.
Schwartz, N., Carminati, A., Javaux, M., 2016. The impact of mucilage on root water uptake-a numerical study. Water Resour. Res. 52 (1), 264–277. https://doi.org/10.1002/2015wr018150.
Schwendenmann, L., Pendall, E., Sanchez-Bragado, R., Kunert, N., Hölscher, D., 2015. Tree water uptake in a tropical plantation varying in tree diversity: interspecific differences, seasonal shifts and complementarity (DOI:doi:). Ecohydrology 8 (1), 1–12. https://doi.org/10.1002/eco.1479.
Simunek, J., Hopmans, J.W., 2009. Modeling compensated root water and nutrient uptake. Ecol. Model. 220 (4), 505–521. https://doi.org/10.1016/j.ecolmodel.2008.11.004.
Sun, Q., Gilgen, A.K., Signarbieux, C., Klaus, V.H., Buchmann, N., 2021. Cropping systems alter hydraulic traits of barley but not pea grown in mixture. Plant, Cell Environ. 44 (9), 2912–2924. https://doi.org/10.1111/pce.14054.
Thomas, A., Yadav, B.K., Simunek, J., 2020. Root water uptake under heterogeneous soil moisture conditions: an experimental study for unraveling compensatory root water uptake and hydraulic redistribution. Plant Soil 457 (1–2), 421–435. https://doi.org/10.1007/s11104-020-04738-3.
Thorup-Kristensen, K., Cortasa, M.S., Loges, R., 2009. Winter wheat roots grow twice as deep as spring wheat roots, is this important for N uptake and N leaching losses? Plant Soil 322 (1–2), 101–114. https://doi.org/10.1007/s11104-009-9898-z.
van Dusschoten, D., et al., 2020. Spatially resolved root water uptake determination using a precise soil water sensor. Plant Physiol. 184 (3), 1221–1235. https://doi.org/10.1104/pp.20.00488.
van Genuchten, M.T., 1980. A closed-form equation for predicting the hydraulic conductivity of unsaturated soils. Soil Sci. Soc. Am. J. 44 (5), 892–898.
Vandoorne, B., Beff, L., Lutts, S., Javaux, M., 2012. Root water uptake dynamics of cichorium intybus var. sativum under water-limited conditions. Vadose Zone J. 11 (3), 16. https://doi.org/10.2136/vzj2012.0005.
Vrugt, J.A., Gupta, H.V., Bouten, W., Sorooshian, S., 2003. A shuffled complex evolution metropolis algorithm for optimization and uncertainty assessment of hydrologic model parameters. Water Resour. Res. 39 (8), 18. https://doi.org/10.1029/2002wr001642.
Wang, D., et al., 2020. Change in hydraulic properties of the rhizosphere of maize under different abiotic stresses. Plant Soil 452 (1–2), 615–626. https://doi.org/10.1007/s11104-020-04592-3.
Williams, D.G., et al., 2004. Evapotranspiration components determined by stable isotope, sap flow and eddy covariance techniques. Agric. . Meteorol. 125 (3–4), 241–258. https://doi.org/10.1016/j.agrformet.2004.04.008.
Xu, J., et al., 2021. Stable oxygen isotope analysis of the water uptake mechanism via the roots in spring maize under the ridge-furrow rainwater harvesting system in a semi-arid region. Agric. Water Manag. 252, 15. https://doi.org/10.1016/j.agwat.2021.106879.
Zarebanadkouki, M., Kim, Y.X., Carminati, A., 2013. Where do roots take up water? Neutron radiography of water flow into the roots of transpiring plants growing in soil. N. Phytol. 199 (4), 1034–1044. https://doi.org/10.1111/nph.12330.
Zhang, X., et al., 2021. Relationship between soil carbon sequestration and the ability of soil aggregates to transport dissolved oxygen. Geoderma 403, 115370. https://doi.org/10.1016/j.geoderma.2021.115370.
Zhang, X.X., et al., 2020. A comparison between water uptake and root length density in winter wheat: effects of root density and rhizosphere properties. Plant Soil.: 12. https://doi.org/10.1007/s11104-020-04530-3.
Zhang, X.X., Bengough, A.G., Crawford, J.W., Young, I.M., 2002. Efficient methods for solving water flow in variably saturated soils under prescribed flux infiltration. J. Hydrol. 260 (1–4), 75–87. https://doi.org/10.1016/s0022-1694(01)00598-4.
Zhou, H., et al., 2020. The interaction between wheat roots and soil pores in structured field soil. J. Exp. Bot. 72 (2), 747–756. https://doi.org/10.1093/jxb/eraa475.
Zuo, Q., Zhang, R.D., 2002. Estimating root-water-uptake using an inverse method. Soil Sci. 167 (9), 561–571. https://doi.org/10.1097/00010694-200209000-00001.
Zuo, Q., Jie, F., Zhang, R.D., Meng, L., 2004. A generalized function of wheat's root length density distributions. Vadose Zone J. 3 (1), 271–277.
Zuo, Q., Shi, J.C., Li, Y.L., Zhang, R.D., 2006. Root length density and water uptake distributions of winter wheat under sub-irrigation. Plant Soil 285 (1–2), 45–55. https://doi.org/10.1007/s11104-005-4827-2.